



Spatial–temporal radiation distribution in a CuBr vapor brightness amplifier in a real laser monitor scheme

L. Li^{1,2} · D. V. Shiyarov³ · F. A. Gubarev¹

Received: 21 April 2020 / Accepted: 30 August 2020 / Published online: 9 September 2020
© Springer-Verlag GmbH Germany, part of Springer Nature 2020

Abstract

The non-uniform gain of the active media is a significant issue in terms of optimizing the beam profile and ensuring image quality of the laser monitor. In this paper, a study of the radial distribution of radiation in copper bromide brightness amplifiers in real schemes of laser monitors is presented. The radial distribution of radiation in a two-pass parallel beam amplified by a brightness amplifier is compared with the radiation distribution in a beam that carries an image in conventional and mirror-imaging laser monitors. The results demonstrate that for metal vapor gain media operated at low concentration of the working substance vapors, the appropriate choice of imaging optics can partially or completely uniform image intensity profile. In case of remote laser monitoring, the intensity dip at the center of the amplified beam completely disappears in the mirror-imaging laser monitor up to a distance of 2 m from the brightness amplifier. This observation range is sufficient for most tasks in the study of the combustion of energetic materials.

1 Introduction

Active optical systems with brightness amplification—laser projection microscopes, originally invented as devices for projecting a large-screen image enlarged and amplified in brightness [1–4], subsequently showed promise in the tasks of visualizing processes accompanied by intense background lighting, such as gas discharges, welding, plasma processes, interaction of laser radiation with matter [5–11]. The plasma layer above the heated surface of a high-temperature object of study creates a screen that impedes observation by conventional visual methods, including using digital video recording. In most cases, the plasma layer is transparent to the radiation of the laser monitor over a wide temperature range [9]. The basis of a laser projection microscope or laser monitor is an active laser medium based on metal vapor, usually copper. To date, the lasers on vapors of copper and

copper compounds, emitting radiation in the visible spectrum at wavelengths of 510.6 and 578.2 nm, have been highly developed [12–19] and have become reliable and relatively compact devices for use in scientific research and technological purposes. In this regard, in recent years considerable attention has been paid to the search for new areas of application for laser monitors. One of the new applications of a laser monitor is its use for studying the surface of aluminum-based metal nanopowders during high-temperature combustion in air [20, 21].

Metal nanopowders, in particular, aluminum-based nanopowders, are materials widely used in industry for the production of ceramic materials and high-energy compounds [22–28]. Combustion of metal nanopowders, in particular, aluminium-based nanopowders and mixtures, takes place at temperatures above 2000 °C, and is accompanied by a bright light emission and in some cases by the scattering of combustion products [22]. Moreover, the combustion process is a fast process with a burning rate of millimeters-centimeters per second. These factors make it difficult to study combusting by visual methods. Unlike other methods, a laser monitor allows to visualize the sample surface of burning nanopowders in real time and estimate combustion characteristics [20, 21].

Laser monitor is a system of visual observation which combines illumination of object under observation by own one-passed amplified spontaneous emission (ASE) and

✉ F. A. Gubarev
gubarevfa@tpu.ru

¹ National Research Tomsk Polytechnic University, 30 Lenin Avenue, Tomsk 634050, Russia

² Liaoning Technical University, 188 Longwanning Avenue, Huludao 125105, China

³ V.E. Zuev Institute of Atmospheric Optics, Russian Academy of Sciences, Siberian Branch, 1 Academician Zuev Square, Tomsk 634021, Russia

amplification of the reflected light [4]. When designing such a system, it is necessary to take into account the effect of the gain nonuniformity of the brightness amplifier radiation on the images that it forms. The light reflected from the object returns to the gain medium with a delay compared to the seeded radiation, which depends on the distance between the object of observation and the brightness amplifier [29]. Therefore, it is necessary to understand how the nonuniformity of the active medium gain radial distribution affects the laser monitor image. In [29] we investigated the dependence of the radial distribution of radiation in the copper bromide vapor amplifiers on the time of the return of their own reflected radiation. It was shown that during the first 7–12 ns without HBr and up to 18 ns with HBr additive, the radiation profile has a distribution close to the Gaussian's one. By the end of the lasing pulse, the profile becomes distinctly ring-shaped. The tubes of 2.5 cm bore, 50 cm length and 5 cm bore, 90 cm length were under investigation in the experiments [29]. Typically, the distance from the gas-discharge tube (GDT) of the brightness amplifier to the object of observation in laser monitors is 15–20 cm, which is in the range when the gain profile does not have a significant dip at the center [29, 30]. In [31], we demonstrated the possibility of using a mirror-imaging scheme to increase the distance to the object of observation. In [32], we used a mirror-imaging scheme together with the conventional scheme of laser monitor to study the surface of metal nanopowders during combustion. Such schemes of a laser monitor with an increased distance to the object of observation are necessary for the remote study of burning powder materials, especially in the cases when a spray of the products accompanies combustion, a significant observation area (several millimeters in diameter) is required, and a high optical magnification is not critical. The long-focus laser monitor scheme used in the recent work [11] for remote monitoring of the process also returns light reflected from the object with a delay relative to ASE.

In the scheme in [32], the distance from the mirror to the object of monitoring was 50 cm at a distance of 1 m from the brightness amplifier to the object. This is the maximum distance for today when observing high-temperature processes using a laser monitor. According to the results of [29], at such a distance to the object, the reflected radiation returns to the gain medium, which already has a slight decrease in gain at the center. Presumably, with a further increase in the distance to the object of observation, the effect of gain nonuniformity will manifest itself. However, today it is not possible to say how significant this effect will be in a real laser monitor scheme. It is not possible to declare, how much the gain dip at the center of the beam in the case of a decrease in the concentration of the vapor of the working substance, which inevitably occurs during long-term operation of a gas-discharge tube, affects the radial intensity distribution of the

brightness amplifier output radiation in laser monitors. The results in [23, 30] were obtained when light rays reflected from a flat mirror propagate almost in parallel. In a real laser monitor scheme, there are imaging optical elements, such as a concave mirror or lens, which form crossed beams that propagate through the amplifying medium non-parallel. The authors are not aware of works in which the radial distribution of gain in laser projection systems with brightness amplification and the influence of the operating conditions of the active element on this distribution would be discussed.

The aim of the present work was studying the effect of gain nonuniformity caused by a decrease in the concentration of working substance vapors and an increase in the distance from the brightness amplifier to the object of observation in a real laser monitor scheme. We also aimed to compare the radial distribution of the output radiation of the brightness amplifier in laser monitors with the radial distribution of a two-pass parallel beam.

2 Experimental

In practical applications, for designing laser monitors and observing objects through plasma, it is sufficient to use brightness amplifiers with an average ASE power of hundreds of milliwatts to units of watts [4–9]. ASE power is especially critical when illuminating the surface of energetic materials, as may cause uncontrolled initiation of combustion [21]. Thus, for the design of imaging systems, it is sufficient to use small-sized GDTs and low-power supplies (less than 1 kW). In this research, we studied the brightness amplifiers, which were used in actual practice to build laser monitors for diagnostic imaging.

We studied two amplifiers with small gain volumes. The first brightness amplifier (BA1) had a GDT with a length of the gain medium of 50 cm and a bore of 1.5 cm. This brightness amplifier we previously used in works [20, 21]. The second amplifier (BA2) had a GDT with a gain medium length of 60 cm and a bore of 3.0 cm [32]. Both GDTs were sealed-off and had an external heater of the gain medium. Heating of the gain medium and containers with copper bromide was provided independently [29, 30]. In this construction of the tube, the copper bromide vapors came into the gain medium by the heating of the containers with copper bromide. The containers were evenly spaced along the length of the GDT. Since the high ASE power was not required and even undesirable for illumination of highly inflammable powders, we did not use HBr active additive into the gain medium, which adding usually leads to significant increasing lasing power [33–36]. The maximum average ASE power registered by the Ophir Orion-PD300 photodetector installed at the site of the object in the conventional laser monitor (Fig. 1a) with an 80 mm lens was 14 mW for BA1 and 22 mW for BA2.

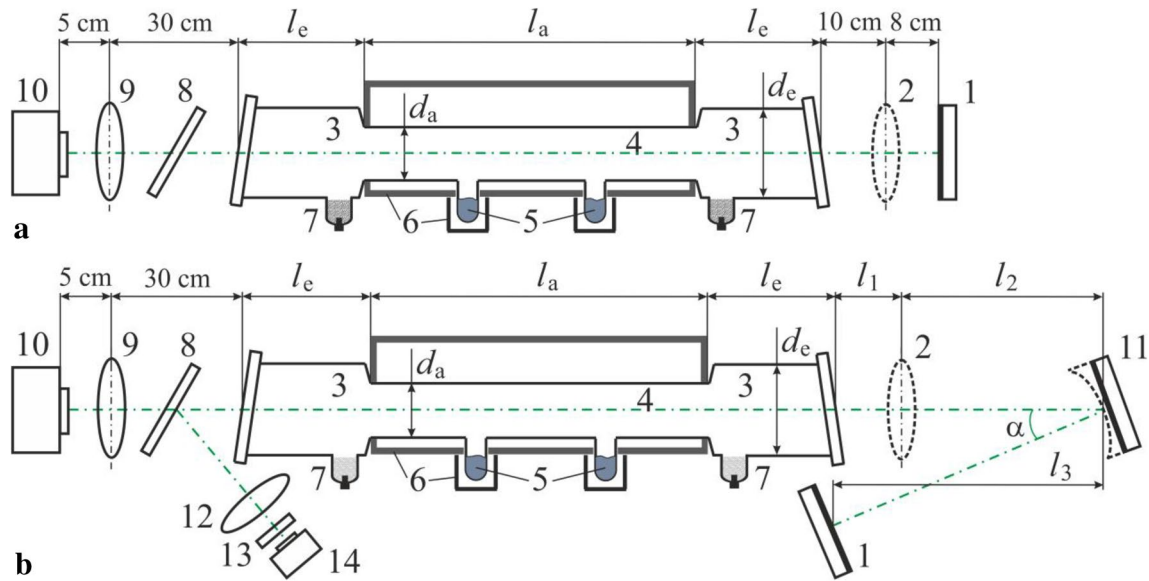


Fig. 1 Schemes of radiation profile registration. **a** Conventional laser monitor short-focus scheme; **b** mirror-imaging laser monitor scheme; 1—flat mirror, 2—lens, 3—end parts of GDT, 4—active part of GDT, 5—CuBr containers, 6—heaters, 7—electrodes, 8—gray filter, 9—

camera coupling lens, 10—high-speed camera, 11—flat (solid lines) or concave (dotted lines) mirror, 12—photodiode coupling lens, 13—diffuser, 14—photodiode

The temperature of the GDTs wall was maintained at a constant level of 660 °C. The temperature of the containers with copper bromide (T_{CuBr}) was set in the range of 455–510 °C for the BA1 and in the range of 475–560 °C for the BA2. The pumping of the brightness amplifiers was performed with a TGI1-500/16 thyratron generator made according to the circuit of direct discharge of the storage capacitor [37] with 750-pF capacitance. The pulse repetition frequency was 20 kHz. The power consumed by the pumping circuit from the DC high-voltage power supply was 600 W.

The experiments were carried out in two configurations of optical schemes, the parameters of which are shown in

Fig. 1 and in Table 1. The first configuration was a conventional short-focus laser monitor scheme (Fig. 1a). The output radiation profile of the brightness amplifier in this scheme was formed using a lens 2 with a focal length of 8 cm (shown by a dotted ellipse) located at a distance of 10 cm from the GDT and a flat mirror 1 with a reflection coefficient of 80% as an object of observation. Using a flat mirror as the object of observation simulates the object with a uniform reflection coefficient throughout the imaging area. When studying the parallel beam profile in this configuration, the lens 2 was removed from the scheme. In some experiments, a test object in the form of a copper

Table 1 GDT and optical scheme parameters

Active part bore d_a , cm	Active part length l_a , cm	End parts length l_e , cm	End parts diameter d_e , cm	GDT-to-object distance in Fig. 1b, cm	GDT-to-lens distance l_1 , cm	Lens-to-mirror distance l_2 , cm	Mirror-to-object distance l_3 , cm
1.5 (BA1)	50	20	4.0	100	10	40	50
				155	90	15	50
				200	140	25	35
				300	245	28	27
				400	345	35	20
3.0 (BA2)	60	30	6.0	80	10	35	35
				130	70	15	45
				195	140	25	30
				300	240	35	25
				400	345	35	20

mesh with a step of 0.3 mm was used as an object of observation. The radiation profile of the brightness amplifier was changed by decreasing the temperature of the containers with copper bromide, i.e. concentration of the working substance in the gain medium.

The second configuration was a mirror-imaging scheme of the laser monitor (Fig. 1b). A mirror-imaging scheme, similar to that used earlier in [31, 32], was assembled by installing a concave mirror 11 with a radius of curvature $R=3$ m (shown by the dotted line) and a lens 2 with a focal length $F=1$ m (shown by the dotted line). A flat mirror 1 modeled the object of study with uniform reflection, as in the first configuration. The mirror was rotated at an angle $\alpha=20^\circ$. When studying the parallel beam profile, the lens 2, indicated by the dotted line, was removed, and the concave mirror 11, indicated by the dotted line, was replaced by a flat mirror. With the optical elements used in the mirror-imaging scheme, it was possible to form a sharp image of the test object (copper mesh) at different distances from the brightness amplifier in five cases of the arrangement of the elements, which are shown in Table 1. Thus, the radial intensity distribution of the output beam of the brightness amplifier in the mirror-imaging and parallel beam schemes was recorded for five distances between the brightness amplifier and the object of observation: 100, 155, 200, 300 and 400 cm for BA1, and 80, 130, 195, 300 and 400 cm for BA2. The temperature T_{CuBr} was kept constant at 510 °C for BA1 and 540 °C for BA2 during all experiments. The temperature of the external wall of both GDTs was maintained at 658 °C, which at a pump power of 600 W provided a lasing mode when the intensity of 578.2 nm wavelength emission was much lower than the intensity of 510.6 nm emission and was almost completely suppressed by the gray filter. Figure 2 presents the emission spectra of the brightness amplifiers recorded by the Avantes AvaSpec-ULS2048-USB2 spectrometer. The spectrometer light guide was located at the place of the high-speed camera.

Using the CMOS camera Phantom Miro C110, we recorded the entire profile of the radiation with a resolution of 1024×1024 pixels and 800 fps rate. The acquired images then were processed using ImageJ software. To provide the registration mode in which the image is formed by a single ASE pulse, synchronizing was performed using a two-channel pulse generator (AKIP-3301) similar to [32]. The generator formed synchronized pulses at frequencies of 800 Hz and 20 kHz, which were fed, respectively, to the synchronization input of the high-speed camera (800 Hz) and the input of external triggering of the thyatron generator (20 kHz). The intensity of radiation was attenuated by gray light filters, which were selected to prevent camera sensor saturation. The gray filter 8 in Fig. 1b also served as a beam splitter for registering the radiation pulse of a brightness amplifier with a photodiode. Simultaneously we registered the lasing pulse of brightness amplifier, the GDT current and voltage using Thorlabs DET10A/M photodiode, Pearson Current Monitor 8450, voltage probe Tektronics P6015A and oscilloscope Tektronix TDS-3054C.

3 Experimental results and discussion

Figure 3 presents the radiation beams images of the brightness amplifiers obtained at different temperatures T_{CuBr} for the cases of a parallel beam (images (1) and (3) for BA1, images (3) and (5) for BA2) and a beam carrying an image in the laser monitor in Fig. 1a [images (1') and (3') for BA1, images (3') and (5') for BA2]. Since the brightness of the images differs significantly depending on the concentration of copper bromide vapors, the patterns are normalized by brightness. The dotted lines show the lines along which the profile was digitized in ImageJ software. Figure 4 shows the radial distribution of the radiation intensity at different temperatures of the containers with the working substance T_{CuBr} . The solid lines indicate the

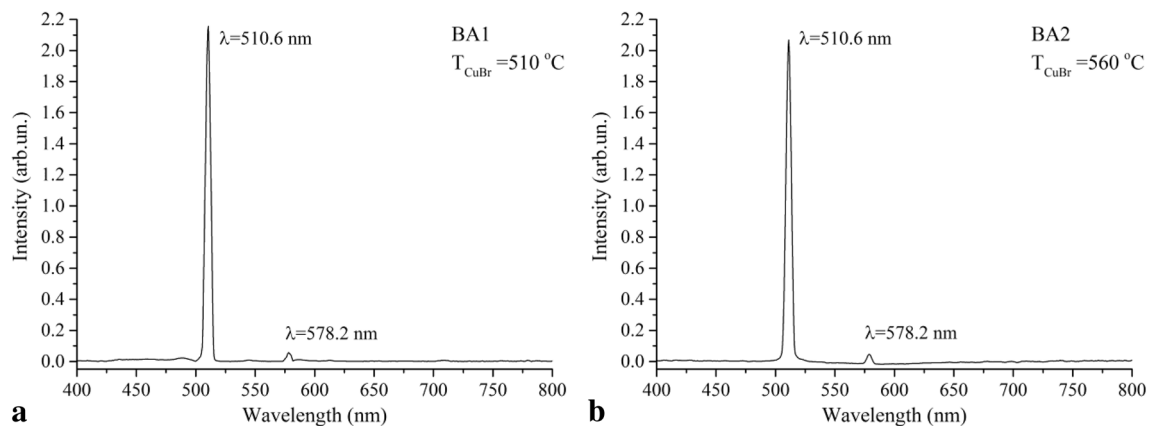


Fig. 2 Emission spectra of the brightness amplifiers BA1 (a) and BA2 (b)

Fig. 3 Brightness amplifier output radiation profiles at different temperatures of copper bromide containers. **a** BA1; 1, 1'— $T_{\text{CuBr}}=510$ °C; 3, 3'— $T_{\text{CuBr}}=475$ °C; **b** BA2; 3, 3'— $T_{\text{CuBr}}=525$ °C; 5, 5'— $T_{\text{CuBr}}=495$ °C; 1, 3, 5—parallel beam, 1', 3', 5'—short-focus laser monitor. The numbers of the figures correspond to the numbers of the curves in Fig. 4 for the corresponding GDTs

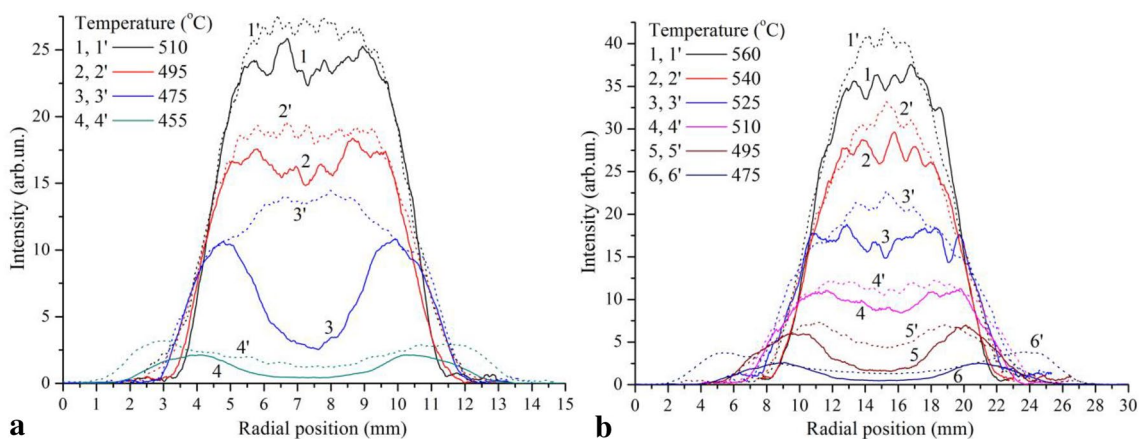
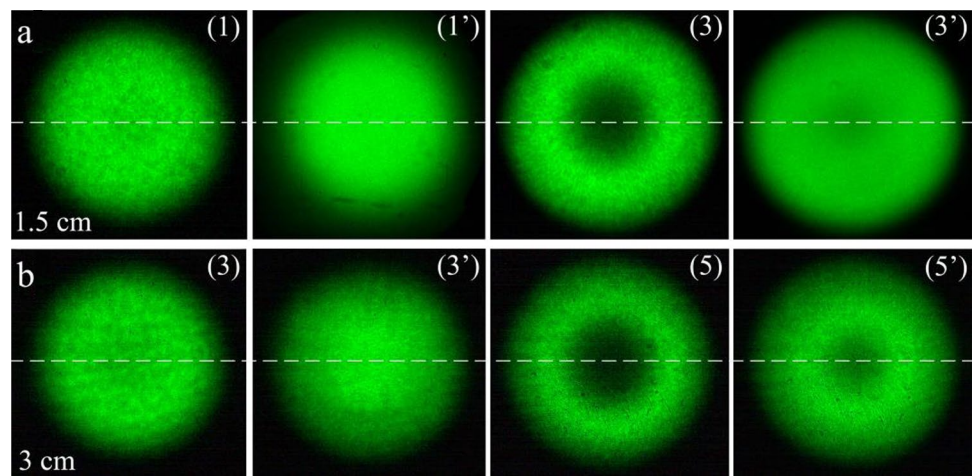


Fig. 4 Brightness amplifier output radiation profiles at different temperatures of copper bromide containers. **a** BA1; **b** BA2. Solid lines 1-6—parallel beams; dashed lines 1'-6'—laser monitor beams

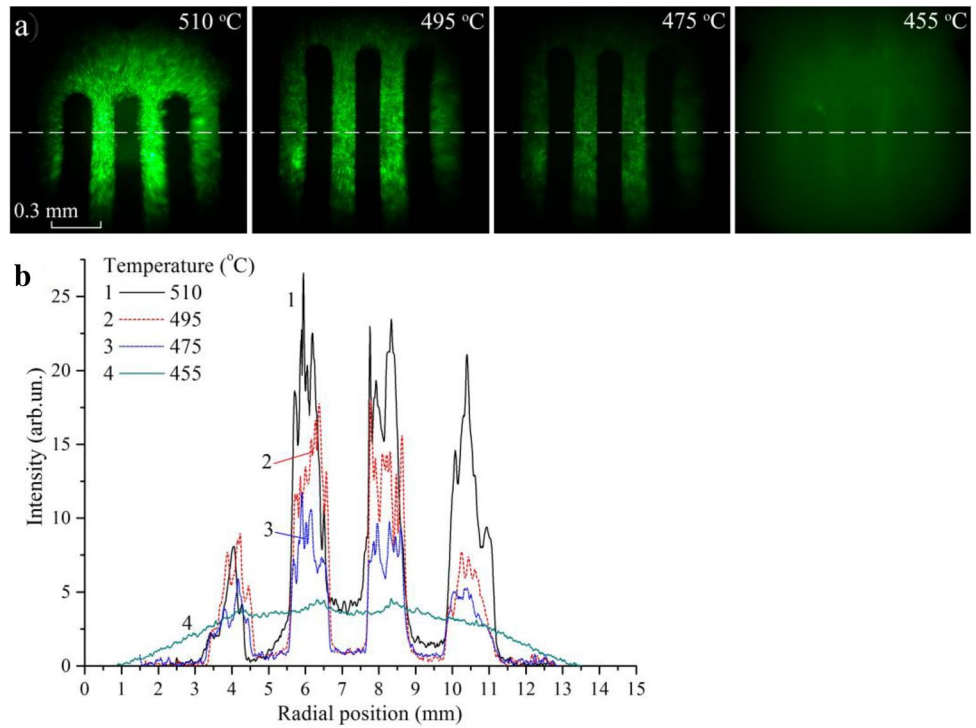
profiles of the amplified parallel beam when the lens 2 is not installed in Fig. 1a. Dashed lines indicate the profile of the beam carrying the image in a real laser monitor scheme when the lens 2 is installed.

From the data presented in Figs. 3 and 4, it follows that the intensity dip at the center of the parallel beam and the formation of an annular beam there are in both GDTs with decreasing temperature T_{CuBr} , similarly to that previously observed in the brightness amplifier with a bore diameter of 5 cm [30]. In contrast to the two-pass amplification of a parallel beam, when the brightness amplifier is operated in a real laser monitor scheme, the intensity at the center of the beam at the same temperature T_{CuBr} is significantly higher. The lack of working substance because of lowering the temperature of the containers, which leads to a significant decrease in intensity at the center of the parallel beam, has a significantly lesser effect in the laser monitor scheme. In particular, the intensity at the center of the amplified beam in the laser monitor scheme (profile 3' in Figs. 3a, 4a) is up to

5 times higher in comparison with the parallel beam (profile 3 in Figs. 3a, 4a).

Figure 5 presents the images of the test object at various temperatures T_{CuBr} . Images brightness falls with decreasing the temperature T_{CuBr} . At $T_{\text{CuBr}}=455$ °C, the image is hardly amplified, in this mode the brightness amplifier is unsuitable for use. In other modes, the image is hard enough for visualization and for quantitative analysis, as shown in Fig. 5b. Thus, in a real laser monitor scheme, the image profile flattens or forms a shape close to Gaussian, even at low gain at the center of the GDT. In our opinion, this is because the image-forming elements, such as lenses and mirrors, in the optical scheme of the laser monitor form the crossing beams that pass through the regions of the GDT both with higher gain and with lower gain. With a decrease in the concentration of the working substance vapors, a gain dip appears at the center of the GDT and ring-shaped radiation is formed when the parallel beam is amplified. When a crossing beam is amplified, light rays pass through both the annular and

Fig. 5 Images of the test object (a) and corresponding intensity profiles (b) at different temperatures of copper bromide containers for BA1



central regions, leading to an increase in the intensity of the output radiation at the center.

In [29], we registered the shift of the amplified-radiation pulse with respect to the ASE of the brightness amplifier when the flat mirror was distanced from the GDT. In GDTs with a bore diameter of 5 cm and a length of 90 cm and a bore diameter of 2.5 cm and a length of 40 cm, the intensity dip at the center of the amplified beam was present already

at a distance of 115–120 cm. A significant drop in the intensity of amplified radiation at the center of the GDT with a bore diameter of 5 cm began when the mirror was distanced farther than 220 cm. Figure 6 shows the waveforms of BA2 pulses for the scheme in Fig. 1b when mirror 1 is distanced. To realize a distance of 200 cm or more between the mirror 1 and the GDT in the experiment, a flat mirror 11 was installed at a distance of 150 cm from the GDT. As follows from the

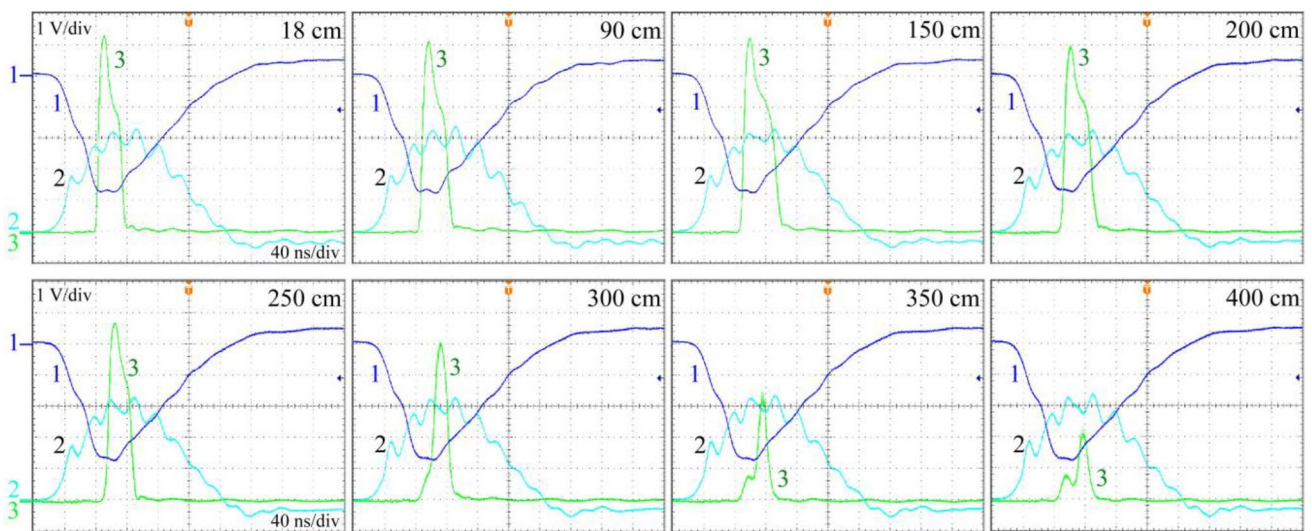


Fig. 6 Waveforms of the brightness amplifier output impulses depending on the distance between the mirror and GDT for BA2. 1—GDT voltage; 2—current; 3—lasing. $T_{CuBr} = 540\text{ °C}$; 600 W pumping power

presented oscillograms in Fig. 6, the voltage and current pulses remain unchanged with high accuracy, which indicates the stable operation of the high-voltage pulsed power supply. When the mirror *I* is distanced from the GDT, a shift of the lasing pulse front to the right with respect to the voltage or current pulse front is clearly observed. Up to a distance of 150 cm, a slight expansion of the lasing pulse occurs, followed by a narrowing. From the presented data, it can be concluded that the use of a laser monitor is possible up to a distance of 2.5 m between the brightness amplifier and the object of observation without a significant decrease in the intensity of images. With a further increase in the distance to the mirror, both the lasing power (i.e., the gain) and the pulse duration decrease. The obtained results are in good agreement with those obtained previously for GDT of a significantly larger size [29].

Figure 7 presents the images of the test object obtained using the mirror-imaging laser monitor for the parameters of

the optical scheme shown in Table 1. Since the parameters of the optical schemes differ, the schemes have different magnification and the field of view. The optimization of optical elements to obtain the clearest image at the given parameters was not the purpose of this study. The main task was to understand how the radiation profile of the brightness amplifier changes when the object of observation is distanced. As follows from the images presented in Fig. 7, there is no visual decrease in intensity at the center. Images are sharp up to the distance of 200 cm. At 300 cm distance, it is still possible to visualize the object, but the image becomes less sharp and there is also significant background radiation. At the distance of 400 cm, the image of the test-object is practically indistinguishable.

In the case of a flat mirror as an object of study, we observe a significant (up to 4.6 times) increase in intensity at the center of the amplified beam compared to a parallel beam (Fig. 8). A parallel beam acquires a dip at the center

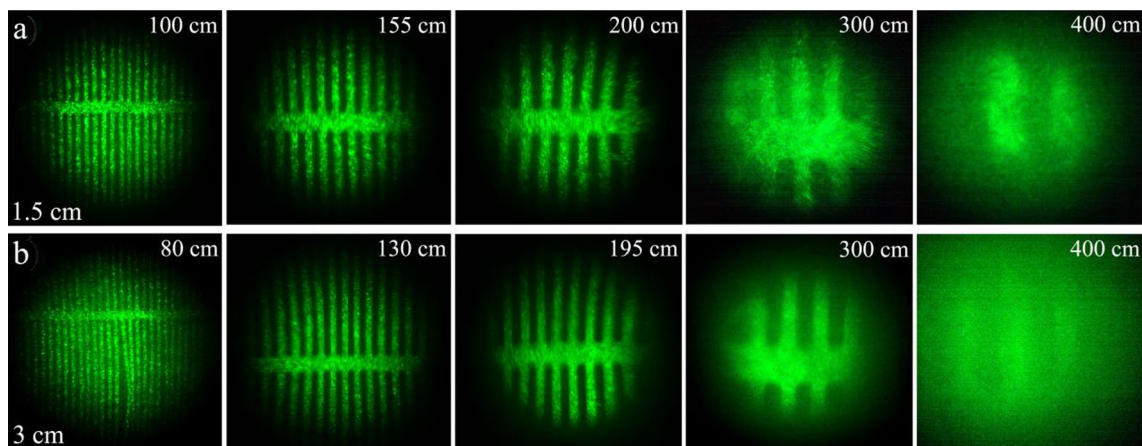


Fig. 7 Images of the test object at different distances between the object and brightness amplifier. **a** BA1; **b** BA2

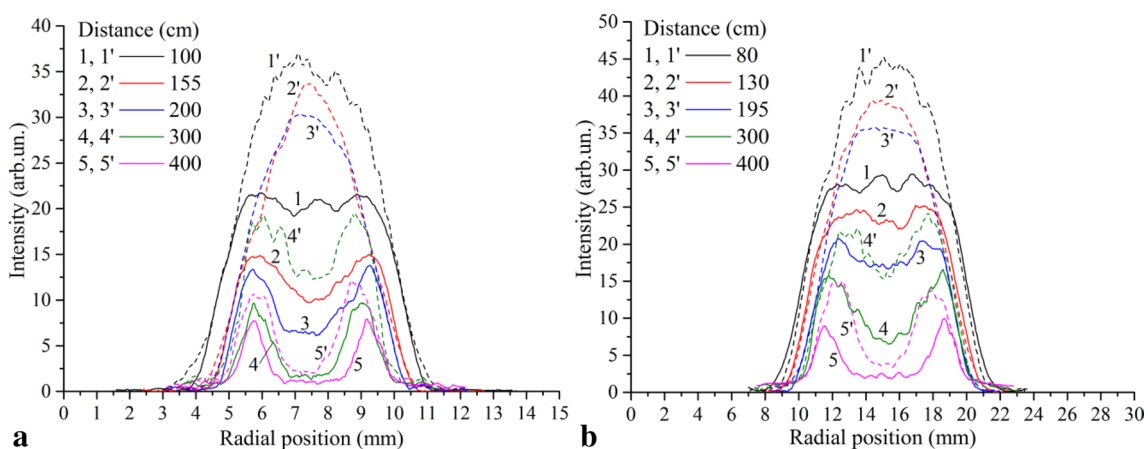


Fig. 8 Brightness amplifier output radiation profiles at different distances. **a** BA1; **b** BA2. Solid lines 1-3—parallel beams; dashed lines 1'-3'—laser monitor beams

as the distance to flat mirror increases, while in the laser monitor the shape of the amplified beam radial distribution remains close to Gaussian. In general, the decrease in the intensity of the brightness amplifiers output radiation in a real scheme is less than when studying a parallel beam. Figure 9 presents the images of the radiation beams of the brightness amplifiers obtained at different distances between the mirror and the GDT for cases of a parallel beam and a beam carrying an image in the mirror-imaging laser monitor in Fig. 1b. Similar to Fig. 3, the patterns are normalized by brightness. Visually, we observe the complete absence of the intensity dip and the maximum brightness at the center of the beams for the distances 80–200 cm. A relatively small dip in the intensity at the center of the beam is observed for the distance of 300 cm. For the distance of 400 cm, the dip in the center is significant both for a parallel beam and for a beam in a real laser monitor.

The appearance of the intensity dip in the case of a parallel beam indicates that at the beginning of the population inversion in the gain medium, the laser beam has a radiation intensity distribution close to a flat top, which then becomes non-uniform with a dip at the center. Obviously, both in the case of a parallel beam and in the case of a crossing beam (mirror-imaging scheme), the radiation enters the active medium with non-uniform gain. Therefore, the presence of image-forming elements in the laser monitor leads to equalization of the gain, integrally along the length of the light rays. Figure 10 depicts simplified diagrams of a parallel beam and an image-carrying beam in a scheme with focusing optics (lens or segmented optics). As shown in the figure, in the case of a parallel beam, the reflected beam is amplified along one radial region (central or near-wall). In a real laser projection system with brightness amplification, the light reflected from an object passes through gain regions with different gain.

Fig. 9 Brightness amplifier output radiation profiles at different distances. **a** BA1; 1, 1'—100 cm; 3, 3'—200 cm; **b** BA2; 1, 1'—80 cm; 4, 4'—300 cm. 1, 3, 4—parallel beam, 1', 3', 4'—mirror-imaging scheme. The numbers of the figures correspond to the numbers of the curves in Fig. 8 for the corresponding GDTs

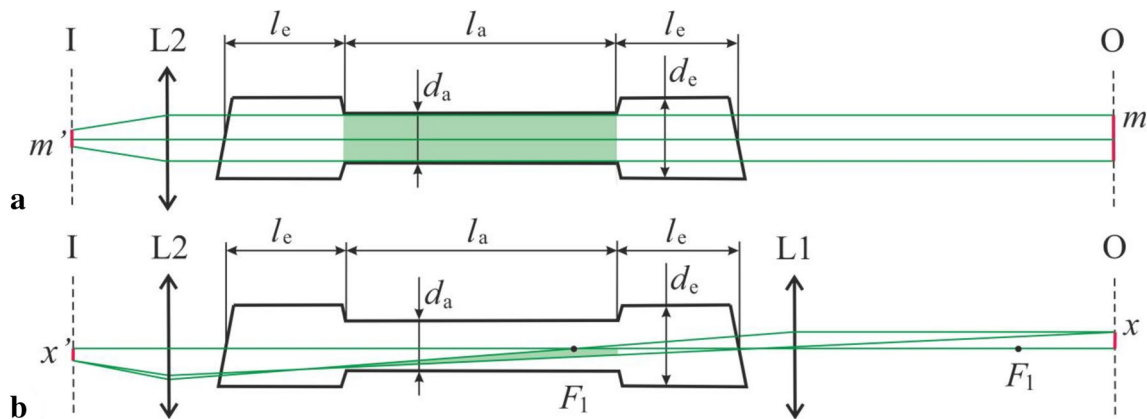
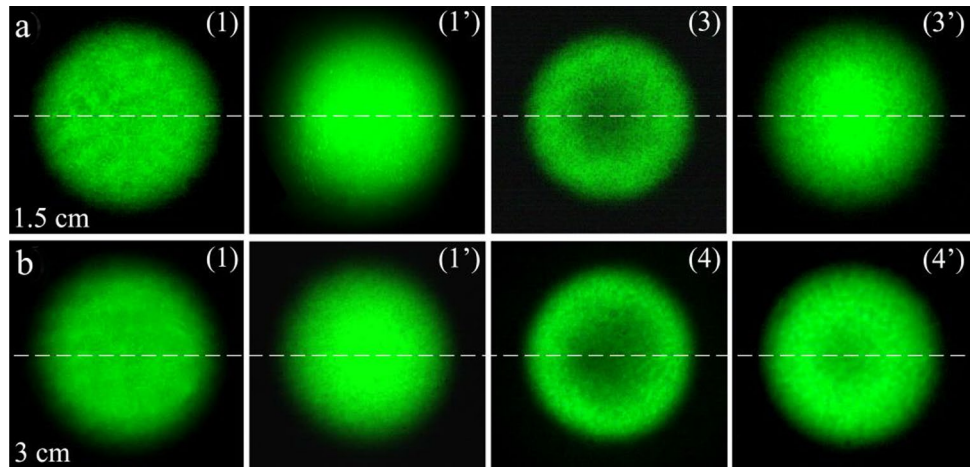


Fig. 10 Simplified ray diagrams of amplification of beams with brightness amplifier. **a** parallel beam; **b** image-carrying beam; O—object plane; L1—focusing optics; L2—camera coupling lens; I—camera matrix plane; m —part of the mirror illuminated by the

parallel beam; m' —image of the amplified parallel beam; x —object; x' —image of the object; F_1 —focal distance. The gain regions are highlighted with green filling

As follows from the data presented in Figs. 8 and 9, gain equalization in the real laser monitor is present in a certain range, which for the used brightness amplifiers is limited to 2–2.5 m. Presumably, for the long-pulse mode of brightness amplifier operation [37] the distance of monitoring can be longer.

4 Conclusions

The paper presents the results of a study of the radial distribution of radiation in beams carrying an image in real laser monitors based on copper bromide vapors brightness amplifiers. The influence of the radial gain nonuniformity present during the lasing pulse, as well as those arising with a decrease in the working substance vapors concentration, is compared for the cases of amplification of a parallel beam and crossed beams formed by optical elements of laser monitors (lenses, mirrors).

In the brightness amplifiers, which are used in actual practice in laser monitors, the profile of the beam carrying an image flattens over the entire operating temperature range of copper bromide containers. Thus, the radial nonuniformity of the gain at the center of the GDT, which occurs when copper bromide vapor concentration is reduced, does not lead to a decrease in the intensity at the center of the amplified beam forming the image of the observation object. This feature makes it possible to operate the GDT of brightness amplifiers in laser monitors almost until the working substance is completely worked-out.

The monitoring range that can be provided by a monostatic laser monitor, that is, using a single brightness amplifier, is limited to 2–2.5 m that is important to bear in view when designing an optical system. In this range, the profile of the beam carrying an image uniforms. At a greater distance, complete uniforming of the profile does not occur. The specified range is caused by decrease in the gain during the lasing pulse and valid for conventional brightness amplifiers with a lasing pulse duration of 30–40 ns (FWHM). In this case, the radial nonuniformity throughout the duration of the lasing pulse, which is observed when the parallel beam is amplified, is completely absent. Presumably, the monitoring range could broaden by implementing the regimes of brightness amplifier operation with prolonged lasing pulse.

These considerations could applied more generally in optical brightness amplifiers. The paper conclusions could equally apply to laser monitors based on different metal vapor gain media where non-uniform gain profiles can be common. For metal vapor gain media operated at reduced temperatures, the appropriate choice of imaging optics can partially or completely uniform image intensity profile.

Acknowledgements The research is carried out at Tomsk Polytechnic University within the framework of Tomsk Polytechnic University Competitiveness Enhancement Program.

References

1. K.I. Zemskov, A.A. Isaev, M.A. Kazaryan, G.G. Petrash, *Sov. J. Quantum Electron.* **4**, 5 (1974)
2. K.I. Zemskov, M.A. Kazaryan, V.M. Matveev, G.G. Petrash, M.P. Samsonova, A.S. Skripnichenko, *Sov. J. Quantum Electron.* **14**, 288 (1984)
3. D.N. Astadjov, N.K. Vuchkov, K.I. Zemskov, A.A. Isaev, M.A. Kazaryan, G.G. Petrash, N.V. Sabotinov, *Sov. J. Quantum Electron.* **15**, 457 (1988)
4. *Optical Systems with Brightness Amplifiers*, ed. by G.G. Petrash (Nauka, Moscow, 1991)
5. V.M. Batenin, I.I. Klimovsky, L.A. Selezneva, *Sov. Phys. Doklady* **33**, 949 (1988)
6. D.V. Abramov, S.M. Arakelyan, A.F. Galkin, I.I. Klimovskii, A.O. Kucherik, V.G. Prokoshev, *Quantum Electron.* **36**, 569 (2006)
7. R.O. Buzhinsky, V.V. Savransky, K.I. Zemskov, A.A. Isaev, O.I. Buzhinsky, *Plasma Phys. Rep.* **36**, 1269 (2010)
8. V.M. Yermachenko, A.P. Kuznetsov, V.N. Petrovskiy, N.M. Prokopova, A.P. Streltsov, S.A. Uspenskiy, *Laser Phys.* **21**, 1530 (2011)
9. G.S. Evtushenko, M.V. Trigub, F.A. Gubarev, T.G. Evtushenko, S.N. Torgaev, D.V. Shiyanov, *Rev. Sci. Instrum.* **85**, 033111 (2014)
10. D.V. Rybka, M.V. Trigub, D.A. Sorokin, G.S. Evtushenko, V.F. Tarasenko, *Atmos. Ocean. Opt.* **27**, 582 (2014)
11. G. Evtushenko, S. Torgaev, M. Trigub, D. Shiyanov, E. Bushuev, A. Bolshakov, K. Zemskov, V. Savransky, V. Ralchenko, V. Konov, *Opt. Laser Technol.* **120**, 105716 (2019)
12. C.E. Little, *Metal Vapor Lasers: Physics, Engineering and Applications* (Wiley, Chichester, 1999)
13. M.J. Withford, D.J.W. Brown, R.P. Mildren, R.J. Carman, G.D. Marshall, J.A. Piper, *Prog. Quantum Electron.* **28**, 165 (2004)
14. D. Astadjov, L. Stoychev, N. Sabotinov, *Opt. Quant. Electron.* **39**, 603 (2007)
15. G.S. Evtushenko, D.V. Shiyanov, F.A. Gubarev, *Metal Vapour Lasers with High Pulse Repetition Rates* (Izd. Tomskogo Politehnicheskogo Univers., Tomsk, 2010)
16. A.N. Soldatov, N.V. Sabotinov, Y.P. Polunin, A.S. Shumeiko, I.K. Kostadinov, A.V. Vasilieva, I.V. Reimer, *Proc. SPIE* **9810**, 981009 (2015)
17. G.N. Tiwari, P.K. Shukla, R.K. Mishra, V.K. Shrivastava, R. Khare, S.V. Nakhe, *Opt. Commun.* **338**, 322 (2015)
18. M.A. Kazaryan, V.M. Batenin, V.V. Buchanov, A.M. Boichenko, I.I. Klimovskii, E.I. Molodykh, *High Brightness Metal Vapor Lasers: Physics and Applications* (CRC Press, Boca Raton, 2017)
19. A.G. Grigor'yants, M.A. Kazaryan, N.A. Lyabin, *Laser Precision Microprocessing of Materials*, 1st edn. (CRC Press, Boca Raton, 2019)
20. L. Li, A.P. Ilyin, F.A. Gubarev, A.V. Mostovshchikov, M.S. Kleynovskii, *Ceram. Int.* **44**, 19800 (2018)
21. L. Li, A.V. Mostovshchikov, A.P. Ilyin, A. Smirnov, F.A. Gubarev, *I.E.E.E.T. Instrum. Measurements* **69**, 457 (2020)
22. V.E. Zarko, A.A. Gromov, *Energetic Nanomaterials: Synthesis, Characterization, and Application* (Elsevier, Amsterdam, 2016)
23. D.S. Sundaram, V. Yang, E. Zarko, *Combust. Explos. Shock Waves* **51**, 173 (2015)
24. S.L. Kharatyan, A.G. Merzhanov, *J. Self-Propag. High Temp. Synth.* **21**, 59 (2012)

25. V.V. Zakorzhevskii, I.P. Borovinskaya, N.V. Sachkova, *Inorg. Mater.* **38**, 1131 (2002)
26. A.V. Mostovshchikov, A.P. Ilyin, I.S. Egorov, *Radiat. Phys. Chem.* **153**, 156 (2018)
27. M.L. Pantoya, J.J. Granier, *Propellants Explos. Pyrotech.* **30**, 53 (2005)
28. K.L. McNesby, B.E. Homan, R.A. Benjamin, V.M. Boyle, J.M. Densmore, M.M. Biss, *Rev. Sci. Instrum.* **87**, 051301 (2016)
29. F.A. Gubarev, L. Li, M.S. Klenovskii, D.V. Shiyarov, *Appl. Phys. B Laser Opt.* **122**, 284 (2016)
30. F.A. Gubarev, M.V. Trigub, M.S. Klenovskii, L. Li, G.S. Evtushenko, *Appl. Phys. B Laser Opt.* **122**, 2 (2016)
31. F.A. Gubarev, L. Li, M.S. Klenovskii, *IOP Conf. Ser. Mater. Sci. Eng.* **124**, 012016 (2016)
32. F.A. Gubarev, S. Kim, L. Li, A.V. Mostovshchikov, A.P. Il'in, *Instrum. Exp. Tech.* **63**, 379 (2020)
33. D.V. Shiyarov, G.S. Evtushenko, V.B. Sukhanov, V.F. Fedorov, *Quantum Electron.* **37**, 49 (2007)
34. V.A. Dimaki, V.B. Sukhanov, V.O. Troitskii, A.G. Filonov, *Instrum. Exp. Tech.* **55**, 696 (2012)
35. A.G. Filonov, D.V. Shiyarov, *Instrum. Exp. Tech.* **56**, 349 (2013)
36. F.A. Gubarev, D.V. Shiyarov, V.B. Sukhanov, G.S. Evtushenko, *IEEE J. Quant. Electron.* **49**, 89–94 (2013)
37. F.A. Gubarev, V.F. Fedorov, K.V. Fedorov, D.V. Shiyarov, G.S. Evtushenko, *Quantum Electron.* **46**, 57 (2016)

Publisher's Note Springer Nature remains neutral with regard to jurisdictional claims in published maps and institutional affiliations.